INSTALLATION OF SUCTION CAISSONS IN SAND

Felipe Villalobos
Universidad Católica de la S^{ma} Concepción
avillalobos@ucsc.cl

ABSTRACT.

Caissons are usually installed by applying suction to its interior. The suction installation imposes a different loading path when compared with the push or jack installation, reflected in the variation of effective stresses around the skirts whose effects need to be investigated. This paper presents results from experiments planned and performed to asses the variables involved in the analysis of caisson installation in sand. Comparisons between measured and calculated results are pursued.

1. INTRODUCTION. The search for improving anchorage systems for military submarine applications led to the idea that an inverted `cup' subjected to vacuum might be a feasible solution (if not the only one) to the anchoring problem as considered by Goodman et al. in 1961. Suction installed skirted footings were not commercially used until 1980 (Senpere and Auvergne, 1982). However, it was in early nineties that extended use in mooring applications for floating production units took place. The first permanent suction caissons were installed in 1995, and nowadays there are more than 485 suction caissons installed worldwide (Andersen et al., 2005). Although, Ibsen et al. (2003) report the suction assisted installation of a 12 m diameter caisson for a wind turbine in Frederikshavn, there is not yet an offshore installation for such an application.

The installation of a caisson by suction is possible due to the generation of a differential pressure between the interior chamber of the caisson and the exterior at the same datum. In practice this differential pressure is obtained by pumping water out of the caisson, which may or may not be submerged. For a submerged caisson the external pressure is hydrostatic, i.e. it varies linearly with the fluid height above the caisson. This differential pressure creates a negative pressure relative to hydrostatic or suction that forces the caisson skirt to penetrate into the ground. There are several factors that need to be considered to make this method of installation successful, e.g. sealing between the soil and the caisson skirt wall, availability, magnitude and limits of the suction, weight of the structure, geometry of the caisson and verticality of the caisson.

This paper starts with the presentation of the installation theory which is based on the work by Houlsby and Byrne (2005). They found that predictions of the suction depend significantly on the combined value of the lateral earth pressure coefficient and friction coefficient, expressed as Ktanδ. Although Houlsby and Byrne gave a range of values obtained from back calculated examples, it is not clear how to chose a certain value from this range or more importantly how to obtain K and δ for any condition. In this paper the calculation of the suction will be based on linear stress distributions.

A comparison between two tests with the same caisson and sand conditions, but installed by pushing and by suction is shown in Figure 1. For the suction installation test the vertical load V' was kept constant at 60 N, and the curve labelled V'+ S represents the net vertical load due to the constant 60 N plus the pressure differential on the caisson lid in terms of force. It is clear that there is a significant reduction of the net vertical load using suction, reflected in the difference between the suction curve and the pushing curve. That difference between these curves represents the beneficial effects of the hydraulic gradients set up within the soil due to the suction.

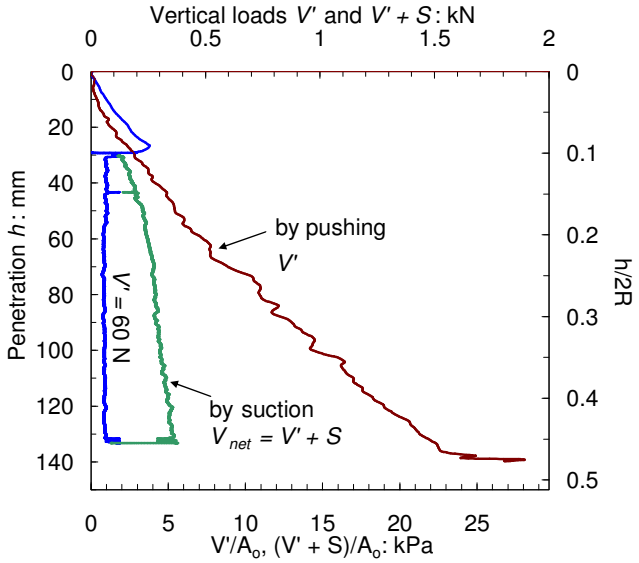

Figure 1: Comparison between pushed installation and suction installation for a 293 mm diameter caisson

2. SUCTION-ASSISTED PENETRATION ANALYSIS. Figure 2 depicts a caisson being penetrated a depth h under the submerged weight V' and the application of suction s, which are counterbalanced by the shear stresses τ_i and τ_o as well as the end bearing stress at the tip σ'_{end}.

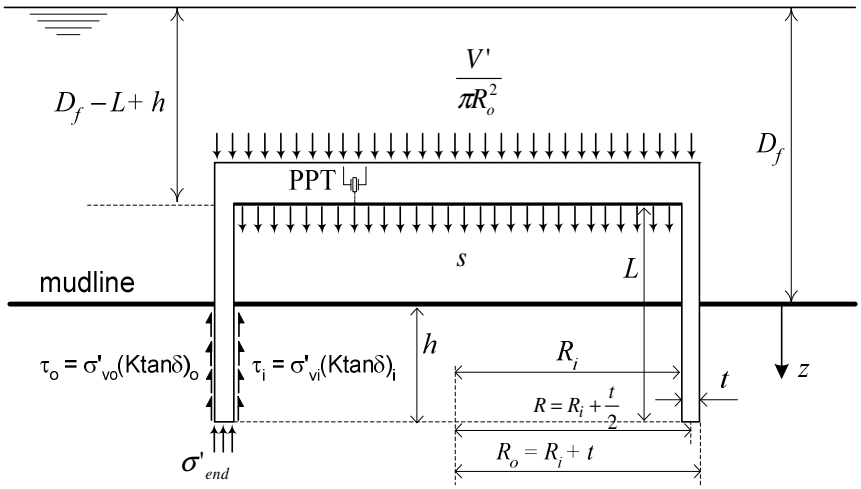

Figure 2: Vertical stresses on a suction caisson during installation

The equilibrium of forces acting on the caisson can be expressed as follows (Houlsby and Byrne, 2005):

$$V' + \underbrace{sA_i}_{S} = \underbrace{2\pi R_o \int_0^h (K_P \tan\delta')_o \underbrace{\sigma'_{vo}}_{\text{seepage}} dz}_{F_o} + \underbrace{2\pi R_i \int_0^h (K_P \tan\delta')_i \underbrace{\sigma'_{vi}}_{\text{seepage}} dz}_{F_i} + \underbrace{(\underbrace{\sigma'_{vi}}_{\text{seepage}} N_q + \gamma' t N_\gamma) 2\pi R t}_{B_q + B_\gamma} \quad (1)$$

where the subscripts o and i refer to outside and inside of the caisson skirt wall respectively. Therefore, R_i and R_o are the inside and outside caisson radii. K_P is the Krynine coefficient of lateral earth pressure, which depends on the soil stress history next to the skirt wall, and tanδ' is the coefficient of friction of the soil-skirt interface with δ' being the interface friction angle. Figure 3(a) shows that owing to friction on the skirt wall soil arching occurs and since by definition principal stresses act only on planes of zero shear stresses σ'_1 and σ'_3 rotate, hence $\theta \neq 90^o$. Taking force equilibrium on a triangular element and deducing $\sigma'_h - \sigma'_3 = \sigma'_1 - \sigma'_v$ from the Mohr circle shown in Figure 3(b), gives (Zeevaert, 1983; Handy, 1985; 2004):

$$K = K_P = \frac{\sigma'_h}{\sigma'_v} = \frac{\cos^2\theta + k_p \sin^2\theta}{\sin^2\theta + k_p \cos^2\theta} = \frac{1 + \sin^2\phi'}{1 - \sin^2\phi'} = \frac{2 - \cos^2\phi'}{\cos^2\phi'} \quad (2)$$

For a smooth wall $\theta = 90^o$, and (2) reduces to the Rankine passive coefficient $k_p = (1 + \sin\phi')/(1 - \sin\phi')$. The Krynine passive pressure coefficient K_P appears for fully mobilised friction at the wall replacing θ by $45^o + \pi/2$.

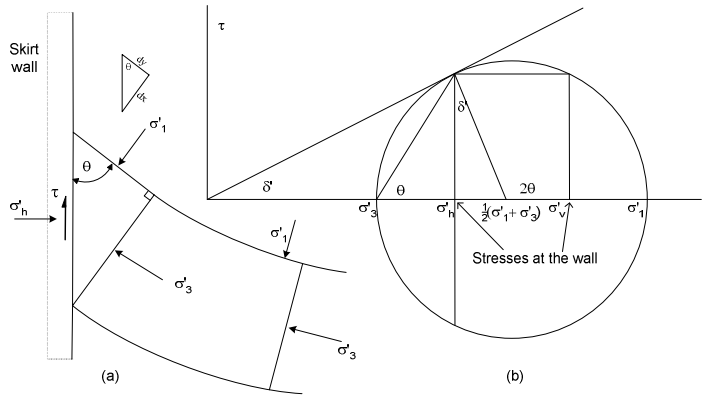

Figure 3: (a) Triangular soil element under force equilibrium showing arching trajectory defined by the minor principal stresses, and (b) Mohr circle showing stresses acting at the wall

The suction s in the left hand side of expression (1) captures the assistance effect in the installation process. The suction creates a flow net which changes the hydraulic head along each flow channel. A schematic flow net is depicted in Figure 4, representing a suction caisson of L/2R = 0.5 and penetrating by suction half of its depth. The flow net has been constructed following procedures for plane strain conditions. For axial symmetric flow nets numerical calculations are necessary. Outside the caisson the downward flow increases the stresses, whereas inside the caisson the upward flow reduces the stresses. Houlsby and Byrne (2005) propose that the change of stresses due to seepage is proportional to the average hydraulic gradients inside and outside the caisson:

$$i_i = \frac{(1-a)s}{\gamma_f h} \quad ; \quad i_o = -\frac{as}{\gamma_f h} \tag{3}$$

where γ_f is the fluid unit weight and a is a pressure factor that represents the ratio between the excess pore fluid pressure at the tip of the caisson skirt and next to the base ($0 \le a \le 1$). Alternatively, the excess pore fluid pressures generated by the seepage regime become a function of the suction and the pressure factor as inside the caisson, and -(1 - a)s outside the caisson. Therefore, the effective vertical stresses in the soil inside and outside the caisson are modified by seepage according to:

$$\underset{\text{seepage}}{\sigma'_{vi}} = \left[1-\frac{(1-a)s}{\gamma' h}\right]\sigma'_{vi} \; ; \quad \underset{\text{seepage}}{\sigma'_{vo}} = \left[1+\frac{as}{\gamma' h}\right]\sigma'_{vo} \tag{4}$$

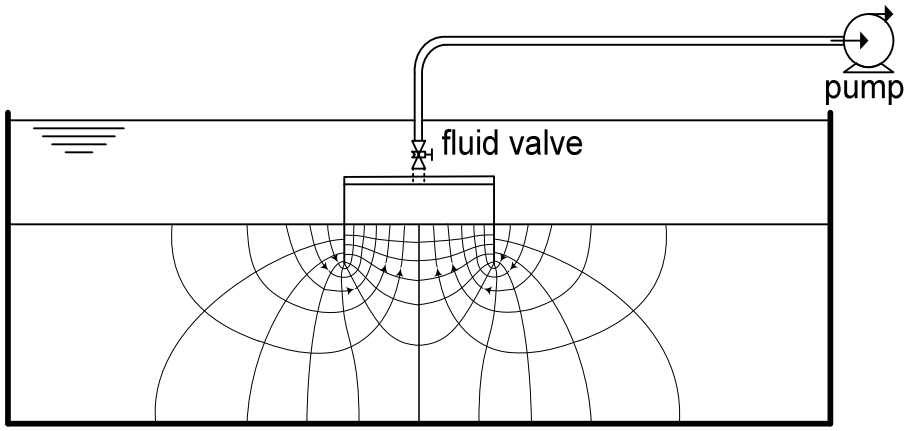

Figure 4: Seepage around a suction caisson during installation

where σ'_{vo} and σ'_{vi} correspond to the case without seepage. The excess pore fluid pressure at the tip of the caisson can be obtained from inside or outside as follows:

$$u' = s - \sigma'_{vi} - \underset{\text{seepage}}{\sigma'_{vi}} = s - \frac{(1-a)s}{\gamma' h}\sigma'_{vi} \quad ; \quad u' = \sigma'_{vo} - \underset{\text{seepage}}{\sigma'_{vo}} = -\frac{as}{\gamma' h}\sigma'_{vo} \qquad (5)$$

which reduces to the distribution –asz/h with depth if $\sigma'_{vi} = \sigma'_{vo} = \gamma' z$. Replacing (4) in the respective σ'_{vi} and σ'_{vo} of expression (1) and solving the integrals results in:

$$V' + sA_i = \pi R_o (K_P \tan\delta')_o \left[\gamma' + \frac{as}{h}\right] h^2 + \pi R_i (K_P \tan\delta')_i \left[\gamma' - \frac{(1-a)s}{h}\right] h^2 + \left[\gamma' - \frac{(1-a)s}{h}\right](hN_q + tN_\gamma) 2\pi Rt \qquad (6)$$

It is worth pointing out that equation (6) reveals that the suction not only contributes as a driving force as in equation (1), but also contributes enormously in reducing the stresses at the caisson tip and inside the caisson next to the skirt. Because of the reduced soil resistance at the caisson tip the skirt penetration is possible under a much lower net vertical load. Alternatively, the suction can be solved from expression (6) resulting in:

$$s = \frac{V' - [\pi R_o (K_P \tan\delta')_o \gamma' h^2 + \pi R_i (K_P \tan\delta')_i \gamma' h^2 + 2\pi Rt\gamma' hN_q + \pi Rt^2 \gamma' N_\gamma]}{ah\pi R_o (K_P \tan\delta')_o - (1-a)[\pi R_i (K_P \tan\delta')_i h + 2\pi Rt(N_q + \frac{t}{h}N_\gamma)] - A_i} \qquad (7)$$

The bracketed expression in the numerator corresponds to the net force required to penetrate a caisson without suction ($F_i + F_o + B_q + B_\gamma$). Multiplying the numerator and the denominator of expression (7) by $\gamma' h$ leads to the introduction of the frictional and bearing capacity forces F_i, F_o, B_q and B_γ in the denominator. In this form a more compact equation for the suction required is obtained:

$$s = \frac{[V' - (F_i + F_o + B_q + B_\gamma)]\gamma' h}{aF_o - (1-a)(F_i + B_q + B_\gamma) - \gamma' h A_i} \quad (8)$$

The pressure factor a accounts for the variation of excess pore pressure with skirt depth. Aldwinkle (1994) carried out a numerical analysis using the finite element program I-DEAS, whereby the seepage problem was solved by means of the heat transfer analogy. The analogies are: conductivity ≡ permeability, and temperature gradient ≡ pressure difference. It was assumed that the reduced `pore pressure' (less negative) at the tip was a times `the suction' in the caisson compartment (T = 0°C); at the same level but outside of the caisson the suction was zero (T = 100°C). The a values obtained by Aldwinkle (1994) covered caisson aspect ratios L/2R ≤ 0.33. Junaideen (2004) (cited by Houlsby and Byrne, 2005) using almost the same mesh details verified and extended the values of a for L/2R ≤ 0.8. If seepage provoked by the suction does not change the soil permeability around the caisson (k_f = 1), then the pressure factor a can be approximated by:

$$a = a_1 = c_0 - c_1\left(1 - e^{-\frac{h}{2Rc_2}}\right) \quad (9)$$

with the values c_0 = 0.45, c_1 = 0.36, and c_2 = 0.48. For a soil permeability ratio $k_f = k_i/k_o$ the pressure factor a is expressed by:

$$a = \frac{a_1 k_f}{(1-a_1) + a_1 k_f} \quad (10)$$

Values of a at h = 0 are not important as this represents just the beginning of penetration before suction would be applied. The fact that seepage can change the soil buoyant unit weight implies also that the void ratio can change, and hence the permeability. The permeability k is found to be related to the void ratio by means of the Kozeny-Carman equation for fully saturated porous media (Mitchell and Soga, 2005), which can be expressed as:

$$k = C_s D_s^2 \frac{\gamma_f}{\mu_d} \frac{e^3}{e+1} \quad (11)$$

where C_s is a shape factor equal to 0.5 if full flow occurs through a tube, D_s can be interpreted as a representative grain size, normally taken as D_{10}; μ_d and γ_f are the viscosity and unit weight of the fluid.

3. EXPERIMENTAL PROCEDURES. The sand used was Redhill 110, whose geotechnical properties are summarised in Table 1. Geologically this sand belongs to the Folkestone beds, which are marine shallow-water deposits of Cretaceous age. It was obtained from Redhill, one of the exposures around the Lower Greensand outcrop in the southeast of England. Commercially produced (WBB Minerals), Redhill 110 is a high silica sand with a total quartz content of 98.8%. Redhill 110 is a fine sand with angular grains, as observed in Figure 5(a). The coefficient of

permeability was estimated by Kelly et al. (2004) to be k = 1.5 $\cdot 10^{-4}$ m/s. Due to this large coefficient of permeability drained conditions are expected.

(a) 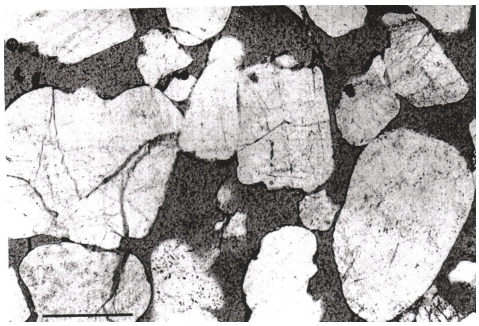

(b) 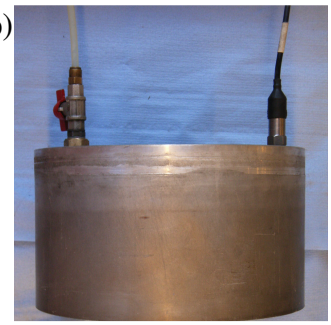

Figure 5: (a) Photomicrograph by Richards and Barton (1999). The scale bar is approximately 0.3 mm in length, and (b) caisson model showing fluid valve and pore pressure transducer

Sand	D_{10} mm	D_{30} mm	D_{50} mm	D_{60} mm	C_u	C_c	G_s	$\gamma_{d\ min}$ kN/m^3	$\gamma_{d\ max}$ kN/m^3	e_{min}	e_{max}	ϕ'_{cs} (^{o})
Redhill	0.08	0.10	0.12	0.13	1.63	0.96	2.65	12.76	16.80	0.547	1.037	36
Luce Bay	0.25	0.31	0.35	0.40	1.60	0.96	2.65	13.54	17.46	0.489	0.920	36

Table 1: Properties of the Redhill 110 sand (Kelly et al., 2004) and Luce Bay sand (Houlsby et al., 2006)

The sample preparation involved deposits of 250 mm height saturated by upward percolation of the water inside a tank of diameter 1100 mm and depth 400 mm. A filter at the bottom together with drainage and a fluid containment tank were set up to aid sample preparation (see Figure 6). Once fully saturated, samples were then densified by vibration with a motor underneath the tank under a small confining stress. A surcharge of 1.5 kPa over a circular plate on top of the sample was used to assist the densification. Above the sand surface a column of water of approximately 130 mm was maintained. To prepare a new sample the process was repeated with the only difference that the fluid in the containment tank was pressurised from the compressor line to create an upward flow which fluidised the sample, instead of gravity used for saturation. The vibration of the tank with the sample in it was halted once a target density was reached. The density was determined by measuring the weight and the volume of the sample.

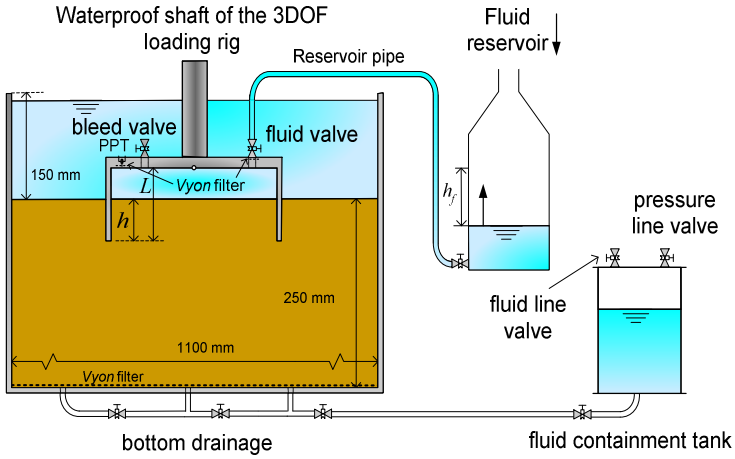

Figure 6: Diagram of the suction device in the laboratory

A water head difference method was used to assist the installation of caissons. Caissons connected to the loading rig arm were pushed into the ground between 15 to 30 mm with the bleed valve open (allowing the pressure inside the caisson to equilibrate with the pressure outside). The bleed valve was closed afterwards, and the fluid valve opened. Fluid in the caisson compartment was connected through a pipe to a reservoir, which was slowly lowered to increase the head difference h_f, between the inside and outside of the caisson. The head difference could be increased to a maximum of 300 mm (3 kPa), whilst the vertical load applied to the footing was kept constant using feedback control in the computer program (Byrne, 2000). The loading rig used was designed and built by Martin (1994).

4. EXPERIMENTAL RESULTS. A summary of the parameters assumed for the suction calculations is listed in Table 2. The first row corresponds to a test carried out in the laboratory and the second and third row correspond to two field trials carried out in Luce Bay, Scotland. For further details of these field trials the reader is referred to Houlsby et al. (2006).

2R: m	L: m	t: mm	V': kN	γ': kN/m^3	R_d: %	ϕ': ^{o}	δ': ^{o}	$K_P \tan\delta'$	k_f	D_f: mm
0.293	0.146	3.4	0.062	10.1	89	46	14	0.8	5	180
1.5	1.0	8	7	10.3	80-85	45	32	2	5	250
3.0	1.5	8	60	10.3	80-85	45	32	2	5	250

Table 2: A summary of parameters used in the calculations of the suction

The values of angle of friction have been estimated using the procedure proposed by Bolton (1986). The interface angles δ' have been assumed according to value ranges presented by Lings and Dietz (2005). Using a direct shear apparatus Lings and Dietz (2005) determine values of δ' between 10.8^o and 13.3^o for a medium sub-rounded sand with relative densities between 23% and 78% and under a normal stress σ'_n of 25 kPa. The surface to which they sheared the sand corresponded to a material with a maximum roughness R_{max} of 3.85 µm. A value of R_{max} around 4 µm was estimated for the aluminium caisson used in the laboratory. Therefore, a compromise value of δ' = 14^o was adopted. For the large caissons used in the field a value of R_{max} = 24 µm as well as a value of D_{50} = 0.35 mm for the Luce Bay sand were assumed. The

previous assumptions result in $\delta' \approx 32^o$ for $R_d = 94\%$ under $\sigma'_n = 25$ kPa according to Lings and Dietz (2005).

The recorded suction underneath the lid with a pore pressure transducer PPT was corrected to obtain the differential pressure, which is the difference between the pressure in the caisson compartment and the pressure in the fluid outside the caisson at the same level, according to Figure 2 the corrected suction results in:

$$s = s_{PPT} - \gamma_f (D_f - L + h) \quad (12)$$

where γ_f is the unit weight of the fluid equal to 9.8 kN/m^3 for water, D_f is the fluid height above the mudline, L is the skirt length and h is the skirt penetration. The range of suction applicable diminishes with D_f, but even if more suction were applied there is a maximum available suction given by:

$$s_{available} = p_a + \gamma_f D_f - p_{cav} \quad (13)$$

where p_a is the atmospheric pressure (≈101.3 kPa) and p_{cav} is the cavitation pressure (≈100 kPa). Therefore, the available suction relies mostly on the fluid height D_f, without which suction is very limited or maybe insufficient to install successfully a suction caisson.

Figure 7 shows a suction-penetration curve measured in the laboratory, where the suction was applied after an initial pushing penetration $h_p = 20$ mm, obtained when V' = 62 N (the calculated penetration for this load is $h_{pe} = 4$ mm). Subsequently, the suction commences under the constant vertical load V' = 62 N that caused the initial pushing penetration. To compare these results with other suction records the non dimensional parameters $s/\gamma'2R$ and $h/2R$ are included in the plots. It is important to highlight that when suction was applied the caisson penetrated vertically without tilting as it may occur under pushing penetration.

The initial pushing penetration of the skirt into dense sand rises a soil plug owing to dilative behaviour. As a consequence of sand dilation an increase of void ratio occurs, hence permeability increases too if the sand is saturated according to the Kozeny-Carman equation (11). In the light of the experimental result this is confirmed, since the soil permeability changes due to dilation and seepage, which modifies the effective stresses during caisson penetration, and as a consequence the void ratio and in turn the permeability ratio k_f is higher than one. This qualitative experimental evidence is supported quantitatively by the suction calculation and equation (11), which relates the increase of permeability with void ratio. Indeed, Figure 7 shows the significant improvement of the suction estimation when a permeability ratio k_f around 5 is chosen. According to these calculation results the predicted suction is strongly dependent on the permeability ratio k_f. A value of $k_f = 1$ lead to a considerable underestimation of the measured suction.

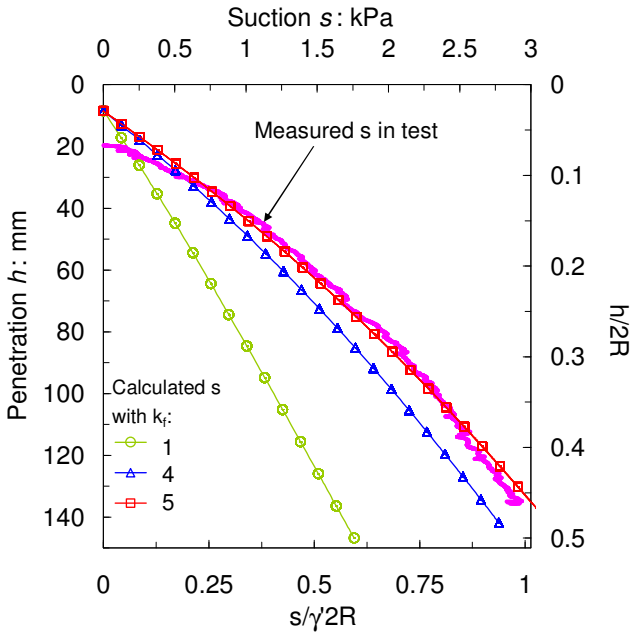

Figure 7: Measured and calculated suction-penetration curves

In the calculations of the suction the surcharge force B_q was predominant whereas the influence of the weight force B_γ was negligible. Finally, the variation of soil permeability cannot be overlooked if an accurate estimation of the suction is pursued. Villalobos (2007) points out that the skirt penetration causes a soil plug heave as a result of dilative behaviour in dense sand. In consequence, soil permeability k_i increases next to the skirt wall since dilation induces the increase of void ratio, but k_o decreases due to the opposite direction of seepage.

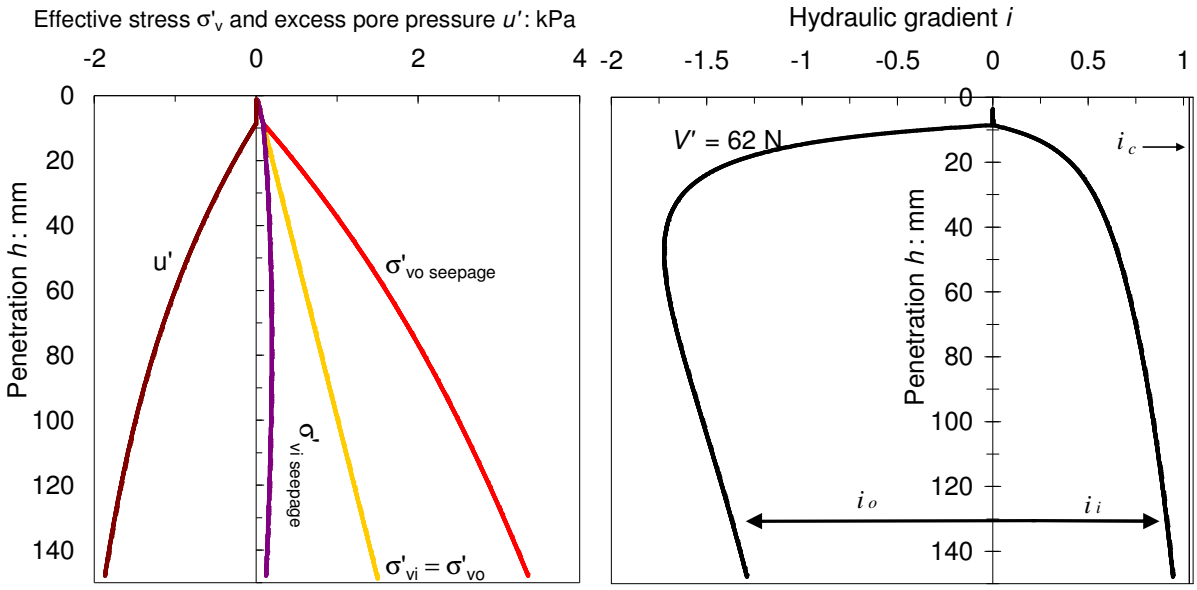

Figure 8: (a) Calculated distribution of effective vertical stresses with and without seepage, and excess pore water pressure u' at the tip of the caisson, and (b) calculated hydraulic gradients inside, outside and critical

Calculated distributions of effective vertical stress are shown in Figure 8(a). Linear distributions of σ'_{vo} and σ'_{vi} correspond to geostatic pressure. The effect of seepage on the stresses is also reflected in Figure 8(a), where the calculated effective vertical stress $\sigma'_{vo\ seepage}$ increased whereas $\sigma'_{vi\ seepage}$ reduced with depth. Furthermore, the calculated distribution of excess pore water pressure u' at the tip of the caisson as penetration occurs is plotted in Figure 8(a). Because the calculation of u' includes the pressure factor a, the distribution of u' is not linear since a varies not linearly with depth. Note the high level of negative excess pore water pressure. The drastic reduction of σ'_{vi} to $\sigma'_{vi\ seepage}$ explains why installation under low net vertical load is possible (Figure 1).

Calculated hydraulic gradients, using equation (3), are opposite in direction yet clear differences in magnitude are found as shown in Figure 8(b). Whilst i_o causes a flow downwards and can be larger than one, i_i causes a flow upwards and has a high initial increase that continues asymptotically. This asymptote corresponds to the critical hydraulic gradient $i_c = \gamma'/\gamma_f = 1.03$, hence $i_i < 1$. A high i_o is beneficial because it strengthens the sand, buffering for instance the spread of an initial piping condition. On the other hand, i_i is also beneficial in the sense that allows the skirt to penetrate under a much lower vertical load. However, i_i is limited by the critical hydraulic gradient i_c, otherwise piping failure may occur and further penetration may not be possible. Figure 8(b) shows that at small penetrations the downward hydraulic gradient i_o is much greater than the upward hydraulic gradient i_i until a maximum value is reached. During subsequent penetration i_o diminishes to values closer to i_i at the end of penetration.

Information from field trials represents an invaluable opportunity to compare laboratory results and calibrate models. Houlsby et al. (2006) have reported a field trial programme in dense sand at Luce Bay. The field trials were designed to install by suction large suction caissons and to subsequently apply monotonic and cyclic load paths. Recordings of the suction measured in the field during installation are shown in Figures 9(a) and 9(b). The data is not smooth as that obtained in the laboratory since the conditions in the field are much harder to control. Since the caissons were not submerged they were filled with water. Under this conditions temporary piping failure is likely to occur from inside to outside as can be seeing in the interruption of the installation, i.e. drop in the suction. Additionally, suction was applied with pumps which were not possible to control. These figures show that predictions of the suction underestimate the measured values. The predictions were carried out assuming a linear distribution of stresses and the parameter values shown in Table 2. Since the caissons were not submerged, V' was modified with caisson penetration.

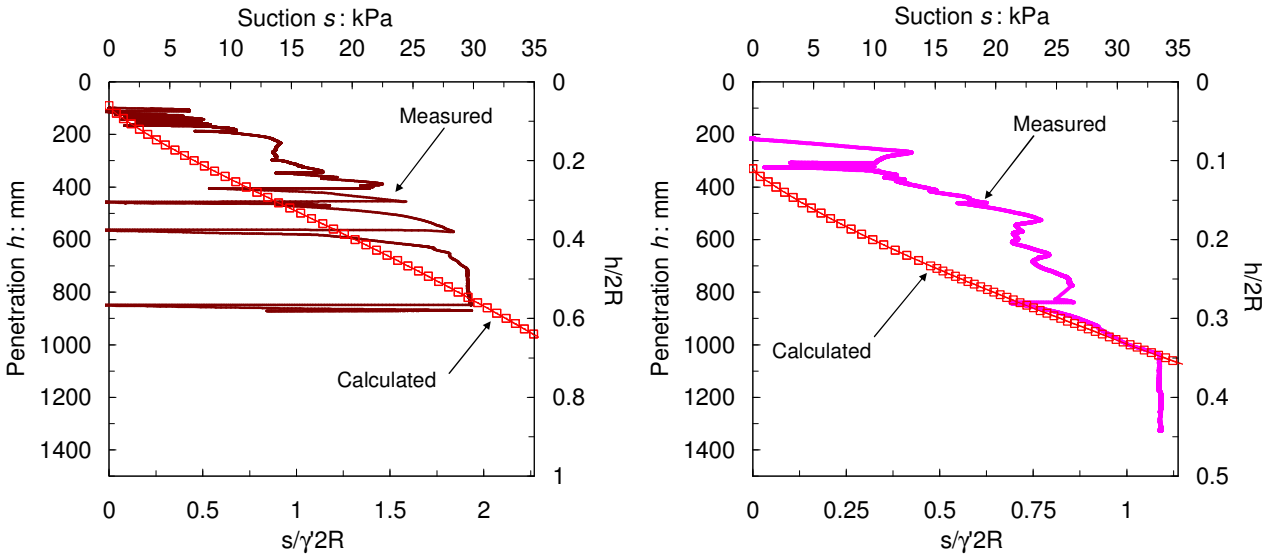

(a) 2R = 1.5 m, L = 1 m, t = 8 mm

(b) 2R = 3 m, L = 1.5 m, t = 8 mm

Figure 9: Measured and calculated suction-penetration curves of field trials

5. CONCLUDING REMARKS.

An expression to evaluate the lateral earth pressure against a frictional wall (not smooth) is suggested. Interface friction angles were correlated by means of the wall maximum roughness. In this way the parameter $K_p \tan\delta'$ could be evaluated and not back calculated.

With the assistance of suction there is a considerable reduction in the net force required to penetrate a caisson into dense sands due to the hydraulic gradients created by the application of suction. In terms of the calculation of the suction the surcharge force was the most relevant followed by the friction forces. The end bearing component is practically negligible.

Seepage generated by the suction influences the soil permeability. It was found that the permeability ratio was decisive parameter in the determination of the suction. A value larger than one was necessary to predict appropriately the experimental results. More research is needed to determine the permeability ratio without back calculations.

It was found that the calculation of the maximum hydraulic gradient i_i was adequate to evaluate the risk of piping or limits to the suction by comparison with the critical hydraulic gradient i_c.

6. REFERENCES.

Aldwinckle, C. G. (1994). The installation of offshore plated foundation for oil rigs. Final Year Project Report, Department of Engineering Science, University of Oxford

Andersen, K.H., Murff, J.D., Randolph, M.F., Clukey, E.C., Erbrich, C.T., Jostad, H.P., Hansen, B., Aubeny, C., Sharma, P. and Supachawarote, C. (2005). Suction anchors for deepwater applications. International Symposium on Frontiers in Offshore Geotechnics, ISFOG, Perth, 3-30

Byrne, B.W. (2000). Investigations of suction caissons in dense sand. DPhil thesis, University of Oxford

Goodman, L.J., Lee, C.N. and Walker, F.J. (1961). The feasibility of vacuum anchorage in soil. Géotechnique **11**, No. 4, 356-359

Handy, R.L. (1985). The arch in soil arching. Journal of the Geotechnical Engineering Division, ASCE, **111**, No 3, 302-318

Handy, R.L. (2004). Anatomy of an error. Journal of Geotechnical and Geoenvironmental Engineering **130**, No. 7, 768-771

Houlsby, G.T. and Byrne, B.W. (2005). Design procedures for installation of suction caissons in sand. Proceedings of the ICE, Geotechnical Engineering **158**, No. 3, 135-144

Houlsby, G.T., Kelly, R.B., Huxtable, J. and Byrne, B.W. (2006). Field trials of suction caissons in sand for offshore wind turbine foundations. Géotechnique **56**, No 1, 3-10

Ibsen, L.B., Schakenda, B. and Nielsen, S.A. (2003). Development of the bucket foundation for offshore wind turbines, a novel principle. Proceeding US Wind Energy Conference, Boston (in `Foundation Engineering Papers', no. 20, 1398-6465, paper no. R0308)

Kelly, R.B., Byrne, B.W., Houlsby, G.T. and Martin, C.M. (2004). Tensile loading of model caisson foundations for structures on sand. International Offshore and Polar Engineering Conference, ISOPE, Toulon, 638-641

Lings, M.L. and Dietz, M.S. (2005). The peak strength of sand-steel interfaces and the role of dilation. Soils and Foundations **45**, No. 6, 1-14

Martin, C.M. (1994). Physical and numerical modelling of offshore foundations under combined loads. DPhil thesis, University of Oxford

Mitchell, J.K. and Soga, K. (2005). Fundamentals of soil behavior. Third edition, John Wiley & Sons, New Jersey

Senpere, D. and Auvergne, G.A. (1982). Suction anchor piles - a proven alternative to driving or drilling. Offshore Technology Conference, Houston, OTC paper 4206

Villalobos, F.A. (2007). Bearing capacity of skirted foundations in sand. Proceedings 6th Chilean Conference of Geotechnics (Congreso Chileno de Geotecnia), SOCHIGE, Valparaíso

Zeevaert, L. (1983). Foundation engineering for difficult subsoil conditions. Second edition, van Nostrand Reinhold